Thermal Hydraulics Design Limits

Class Note II

9/7/06

Professor Neil E. Todreas

The following discussion of PWR steady state and transient design limits is extracted from the theses of Carter Shuffler and Jarrod Trant while the BWR discussion is extracted from Paolo Ferroni's thesis (covers steady state only). These limits are a simplified and narrower discussion than the relevant NRC standard review plan you will also be referred to.

All materials are directly extracted from these theses so that the cited references which appear in this note must be tracked if you have interest by going to the relevant theses.

PWR Steady State Limits

2.1.2.1 MDNBR

Departure from nucleate boiling (DNB) is the most limiting constraint on power for commercial PWRs. DNB occurs at the critical heat flux, which is a function of the geometry and operating conditions in the core. It is characterized by a sharp decline in the heat transfer coefficient at the coolant/cladding interface, as vapor blankets the fuel rod preventing fluid from reaching its outer surface. The result is an abrupt rise in the temperature of both the fuel and cladding, which can damage the fuel and/or cause a cladding breach.

The performance metric for DNB is the MDNBR, which is the minimum ratio of the critical to actual heat flux found in the core. In commercial design, significant margin exists in the MDNBR limit to account for transients, core anomalies (i.e, rod bow), process uncertainty (i.e, instrument error), and correlation uncertainty. While it is difficult to quantify the magnitude of each, a reasonable MDNBR limit can be obtained by executing VIPRE at the reference core geometry and operating conditions. The reference core's MDNBR limit already accounts for the needed margin. The use of the MDNBR given by VIPRE as the MDNBR limit for the steady-state thermal hydraulic analysis therefore ensures that all new designs will demonstrate the same level of DNB margin as the reference core. This limit is ~ 2.17.

One final note on the MDNBR limit is warranted. Using the limit, as described above, assumes that the margins built into the reference core's MDNBR limit are sufficient for all geometries considered in this study. This may not be true, however, for the transient contribution. Consider, for example, the loss of flow accident (LOFA). Designs that are tighter than the reference core will coast down more quickly, and therefore require additional margin for transients in the overall steady-state MDNBR limit. To account for this, a fellow graduate student at MIT, Jarrod Trant, is evaluating the maximum power with respect to specific transient design limits [3]. Ultimately, the final maximum achievable power will be the minimum power given by either the steady-

state or transient analyses, at each geometry. The transient and steady-state results are combined in Chapter 4 of this report for the final economic optimization.

Also note that because the equivalence of full core square and hexagonal thermal hydraulic models is undertaken in this chapter, the limits listed in Table 2.2 are assumed to apply equally to both configurations. The correlation used in VIPRE to determine the CHF is the W-3L, which can be used for both arrays if grid spacers are used. If wire-wrapped designs are considered in the future, new CHF correlations will apply and the MDNBR limit will need to be modified. This is not undertaken in this study.

2.1.2.2 Pressure Drop

The maximum pressure drop sustainable through the primary system is determined by the capacity of the coolant pumps. Two separate pressure drop limits are used in the steady-state thermal hydraulic analysis to reflect the current and 5 year expected enhanced states of pumping technology. While losses occur throughout the entire primary coolant loop, the limit is based on the pressure drop across the fuel bundle, because it will vary most among the redesigned cores.

The lower pressure drop limit indicative of current PWR pumping capacity is determined in the same manner as the steady-state MDNBR limit: finding the pressure drop across the fuel bundle given by VIPRE for the reference core geometry and operating conditions. This pressure drop is approximately 29 psia. The enhanced pressure drop limit is based on examination of pumping capacities for the Westinghouse AP600 and AP1000 PWR designs, and a survey of industry experts. The pressure drop in the core nearly doubled between the design of the AP600 and AP1000, and so it is reasonable to believe that in the next 5 years before a hydride fueled core could be constructed, the capacity could again double. The enhanced fuel bundle pressure drop limit is therefore 60 psia. The maximum power is presented for both pressure drop limits in Section 2.2.

2.1.2.3 Fuel Temperature

Based on experience with hydride fuels used in TRIGA reactors, a steady-state fuel centerline temperature limit of 750 C was adopted for this analysis [1]. The limit is based on prevention of hydrogen release from the fuel during steady-state irradiation. Excessive hydrogen release can embrittle the clad, pressurize the fuel pin, and introduce an explosive hazard into the core. At temperatures below 750 C, the partial pressure of hydrogen gas is low, and the gas remains evenly distributed in the fuel matrix.

Unlike hydride fuels, oxide fuels release non-negligible amounts of fission gas, which, if not limited, can pressurize and even burst the fuel pin. Based on fuel performance data for oxide fuels, the fission gas release fraction can be kept below 5% by limiting the average fuel temperature to 1400 C [4]. This is the temperature limit adopted for oxide fuel. Note that this is more limiting than imposing a peak centerline temperature limit of 2800 C, which is the melting point of UO_2. Note that this temperature limit only applies to steady-state operation; J. Trant's thesis [3] will determine if core designs from the steady-state analysis exceed temperature limits during transients.

2.1.2.4 Axial Flow Velocity

Because the enthalpy rise across the core is fixed, a specific geometry can only achieve higher powers by increasing the coolant flow through the core. As the bulk flow gets larger, the turbulent axial and cross-flow velocities increase, making a vibration-related rod failure more probable. It is therefore desirable to provide design limits to restrict rod vibrations, and resultant wear at the cladding/rod support interface.

In lieu of a detailed vibrations and wear analysis for each core design, J. Malen imposed a single limit on the hot channel axially averaged velocity. The limit was based on a judgment during the initial phase of the Hydride Fuels Project that vibration problems could be avoided in PWRs by limiting the axial velocity of coolant to 7 m/s. The limit adopted was 8 m/s, under the assumption that additional grid spacers would be

added if deemed necessary by a separate fluid-elastic instability analysis of select, optimum geometries.

The wide range of geometries considered and the large power increases reported by the thermal hydraulic analysis makes it prudent to refine this single limit approach. A more thorough analysis of relevant vibration and wear mechanisms is required. This analysis is performed in Chapter 3 of this report. Because the purpose of Chapter 2 is to update J. Malen's results for steady-state maximum power, and to prove the equivalence of hexagonal and square array designs, the single velocity limit is maintained. The final thermal-hydraulic results used in the economic optimization study in Chapter 4, however, will be based on the updated vibrations and wear design limits presented in Chapter 3.

3. Vibrations Analysis for Hydride and Oxide Fueled PWRs

3.1 Introduction

Dynamic forces generated by the turbulent flow of coolant in PWR cores cause fuel rods to vibrate. Flow-induced rod vibrations can generally be broken into two groups: large amplitude "resonance type" vibrations, which can cause immediate rod failure or severe damage to the rod and its support structure, and smaller amplitude vibrations, responsible for more gradual wear and fatigue at the contact surface between the fuel cladding and rod support. While the former group is typically prevented by adequate structural design of the fuel assembly, the latter is unavoidable. Sufficient wear resistance must therefore exist in the fuel assembly components to preclude excessive damage. Ultimately, both vibration types can result in a cladding breach, and therefore must be accounted for in the thermal hydraulic design of hydride and oxide fueled PWRs.

The thermal hydraulic analysis to determine the maximum achievable power for hydride fueled cores did not account for specific vibration mechanisms; instead, a single limit on the axial flow velocity was imposed [1]. This limit was based on a judgment during the initial phase of the Hydride Fuels Project that vibration problems could be avoided in PWRs by limiting the coolant axial velocity to 7 m/s in the core. The wide

range of core geometries considered and the large power increases reported by the thermal hydraulic study makes it prudent to refine this single limit approach. A more thorough analysis of relevant vibration and wear mechanisms is needed, with appropriate design limits imposed for each mechanism.

3.2 Work Scope

3.2.1 Goals of the Vibrations Analysis

The thermal hydraulic analysis for hydride fueled PWRs linked a series of student developed Matlab programs and the VIPRE sub-channel analysis code to iteratively determine the maximum achievable power for a range of core geometries, subject to user defined design constraints. Constraints included minimum departure from nucleate boiling ratio (MDNBR), fuel centerline temperature, bundle pressure drop, and axial flow velocity. The maximum power reported by the study for a given geometry was the highest power for which no constrained parameter exceeded its design limit.

The goal of the vibrations analysis is to develop and incorporate new design limits for flow-induced vibration and wear mechanisms into the existing thermal hydraulic programs, replacing the single limit on axial velocity. The results will include new maps of steady-state power for PWR geometries utilizing hydride and oxide fuels. Combined with the transient analysis performed by J. Trant [3], the thermal hydraulic analysis for maximum power will be complete.

3.2.2 Flow-Induced Vibration Mechanisms - Overview

Three primary types of flow-induced vibration are observed for cylindrical fuel elements subject to cross and axial flow:

- *Vortex-Induced Vibration:* Vortex-induced vibration can occur by two means: vortex shedding lock-in and vortex-induced acoustic resonance. In vortex shedding lock-in, the frequency of the vortices shed by cross-flow over the fuel rod "lock in" to the rod's structural frequencies, causing resonant vibration. In vortex-induced acoustic resonance, the shedding frequency

excites standing acoustic waves created by the operation of fans, pumps, valves, etc. in the coolant loop[1]. Because the rules to avoid lock-in are more conservative than the rules to avoid acoustic resonance, only vortex shedding lock-in is considered in this analysis.

- *Fluid-Elastic Instability:* Fluid-elastic instability of a rod bundle occurs when the cross-flow velocity exceeds the critical velocity for the bundle configuration, at which point the rod response increases uncontrollably and without bound.

- *Turbulence-Induced Vibration in Cross and Axial Flow:* The fluctuating pressure fields generated by cross and axial flow turbulence in the core exert random forces on the fuel rods, causing vibration.

The vibration amplitudes associated with vortex shedding lock-in and fluid-elastic instability are generally very large, and can quickly cause severe damage to the fuel rod and its support structure. If the pitch is tight enough, rod failure by tube-to-tube impaction is also possible. Fortunately, these devastating mechanisms can be prevented by adequate design of the fuel assembly structure for the flow conditions in the core (i.e. using an appropriate number of grid supports and providing adequate stiffness to the fuel rod).

Unlike vortex shedding lock-in and fluid-elastic instability, turbulence-induced vibration is generally of small amplitude and cannot be avoided. The principle design concern is therefore not the prevention of the vibration mechanism, but the limitation of resultant wear at the cladding/rod support interface. Wear is a concern for two reasons. First, excessive wear can directly breach the clad or increase the likelihood of a breach from other rod damage mechanisms (i.e. impact stress and fatigue). Second, wear at the

[1] Standing waves are required for the acoustic resonance condition. They are formed when acoustic waves traveling in opposite directions (as when an acoustic wave deflects off of fuel rods) superimpose onto one another.

cladding/rod support interface lowers the structural frequencies of the rod, making it more susceptible to vortex-induced vibration and fluid-elastic instability.

The most common wear mechanism, and historically the most costly flow-induced vibration problem in the nuclear industry, is fretting wear. Fretting results from combined rubbing and impaction between the fuel rod support and the cladding surface. Sliding, or adhesive, wear also occurs where the grid support springs and rod rub against one another. Both wear types are considered in this study.

The mechanisms considered and their respective design concerns are summarized in Table 3.1.

Table 3.1 Flow-Induced Vibration Mechanisms

Flow-Induced Mechanism	***Design Concern***
Vortex-Induced Vibration	• Large amplitude vibrations occur when vortex shedding frequencies lock-in to the structural frequency of the rod
Fluid-Elastic Instability	• Large amplitude vibrations occur when cross-flows exceed the critical velocity for the rod bundle configuration
Turbulence-Induced Vibration in Cross and Axial Flow	• Small amplitude rod vibrations from turbulence generated pressure fields cause excessive fretting and sliding wear at the cladding/rod support interface

PWR TRANSIENT LIMITS

The second step in the nominal full power method is a transient analysis. The transients to be considered for this study include a loss of coolant accident (LOCA), an overpower transient, and a loss of flow accident (LOFA). The LOCA and overpower transient will each yield the maximum achievable power for the given condition over the entire range of geometries. The maximum achievable power for each of these two transients as well as the initial steady state maximum power will be compared and the minimum power at each geometry will be obtained. These values are then also compared to the rod vibration limits [4] to yield the maximum achievable power for the complete steady state, LOCA, and overpower limits. This data will then be used by C. Shuffler to determine the most economical hydride and oxide cores.

The LOFA transient will then be applied to the most economic cores to verify that they meet the LOFA constraints. This limited assessment of core geometries for the LOFA is necessitated by the fact that there exists no method for determining the viability of specific core geometries without performing a complicated full core analysis. Any of the cores investigated that do not meet the LOFA constraints will be adjusted. These final cores will be the most economic cores based on all previously mentioned steady state and transient limits.

The nominal full power method will be performed for both hydride and oxide fuel for both the 29.0 and 60 psia pressure drop cases. The maximum achievable power of these cores will be compared to the reference oxide fueled core power of 3800 MW_{th} as well as comparing the single highest power hydride fueled core to the single highest power oxide fueled cores over the geometry range. In addition the two fuel types will be compared at each pressure drop case over the range of P/D ratios but at the reference oxide core pitch (12.98 mm) in order to cover a small scale backfit of existing core designs.

Loss of Coolant Accident

The first transient to be considered is the loss of coolant accident (LOCA). There are two types of LOCA events that could be considered. The large break LOCA (LBLOCA) is an

ANS condition IV transient, while the small break LOCA is an ANS condition III transient. The large break LOCA, being more restrictive, will be considered here.

A full scale LOCA evaluation over the entire design range is impractical. However, using the methodology of Catton, et.al [5] will allow use of the clad temperature history of the reference core as the bounding criteria for the entire range of geometries.

Overpower Transient

The second transient to be considered is an overpower transient. There are two ANS Condition II overpower transients which are considered in the South Texas Project Electric Generating Station (STPEGS) Final Safety Analysis Report (FSAR).

The first event is concerned with a main steam line break at power. The second event is rod bank withdrawal at power and the limit challenged is the minimum departure from nucleate boiling ratio (MDNBR).

The main steam line break overpower transient is constrained by the plant's 22.45 kW/ft linear heat rate limit. The rod withdrawal transient is limited by the 18% limit. This 18% overpower limit equates to a 16.03 kW/ft linear heat rate. Therefore, when considering a generic overpower transient, the 16.03 kW/ft limit will be breached prior to the 22.45 kW/ft limit. Therefore, the rod withdrawal will be treated here to cover both overpower transients over the entire geometry range. The limiting condition will be defined as the MDNBR of the reference core for this overpower transient.

Loss of Flow Accident

The third transient, the loss of flow accident, also consists of two categories, the complete loss of flow (CLOFA) and the partial loss of flow accident (PLOFA). The complete loss of flow is more limiting and will be considered here. The CLOFA is an ANS Condition III transient; however, in this paper as well as in the STPEGS FSAR the Condition II limits will be applied.

As with the LOCA, the CLOFA is a complicated transient which is highly dependant upon core geometry. Unlike the loss of coolant accident, there exists no method for

determining the viability of specific core geometries without performing a complicated full core analysis.

As such, the LOFA will not be examined over the entire range of geometries. Instead the output from the steady state, overpower, and LOCA analysis will be used in an economic study performed by C. Shuffler to determine the most economical hydride cores. These specific cores will then be analyzed for the CLOFA. This will provide the most economical hydride and oxide cores for both pressure drop cases for the steady state, overpower, LOCA, and LOFA limits.

This complete nominal full power methodology is outlined in figure 2.1.

Figure 2.1: Complete Nominal Full Power Methodology Outline

1. Initial steady state maximum achievable power as determined by J. Malen [2]
2. Revised steady state maximum achievable power as determined by C. Shuffler [4]
    - Replaces the generic flow velocity limit with a more specific set of rod vibrations criteria
    - Adjusts the range of rod diameters due to initial physics and economic concerns
3. Perform overpower transient analysis
    - Determines the maximum achievable power considering an overpower transient
4. Perform LOCA anlaysis
    - Determines the maximum achievable power considering a LOCA
5. Specify the most economic cores, as determined by C. Shuffler [4]
    - Based on all previous work as well as physics limitations and other economic constraints
6. Perform LOFA analysis on specified economically desirable core geometries
7. Repeat previous steps for both oxide and hydride cores for both pressure drop cases
8. Make final comparison to determine the optimal hydride core geometry considering all outlined steady state, transient, and economic constraints

Transient Methodology

The first step in analyzing each transient involves applying the relevant transient to the reference core geometry. The overpower and LOFA transients use the MDNBR of the

reference core under each condition as the limiting criteria. The LOCA uses the clad temperature history of the reference core as the limiting criterion.

Applying the LOFA and overpower transient to the reference core will provide the Safety Analysis Limit MDNBR ($MDNBR_{S.A.L., REF}$) as shown in figure 2.2. This Safety Analysis Limit MDNBR will be the minimum MDNBR for all cores for the specific transient before applying the "Margin for Transients".

Figure 2.2: Separated Components of Margin for MDNBR

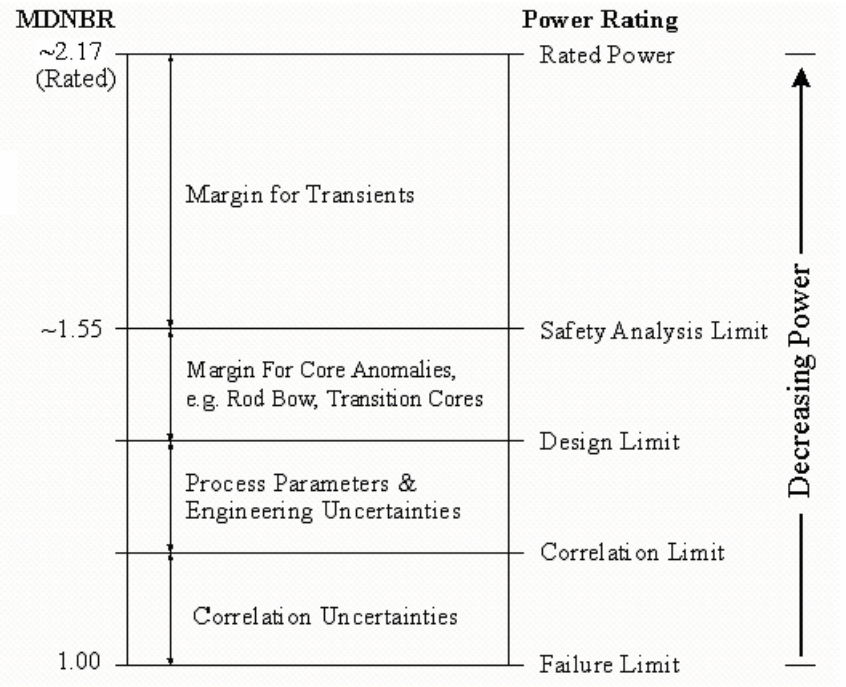

First, the overpower transient will be carried out in a similar manner as the steady state analysis. The maximum power will be determined over the entire geometry range such that the Safety Analysis Limit MDNBR ($MDNBR_{S.A.L}$) of each core does not go below that of the reference core as well as meeting the other steady state limits (flow velocity, pressure drop, and fuel centerline temperature).

The LOCA will then be applied to the reference core to determine the clad temperature over time of the reference core during a LOCA. The LOCA will then be applied to the results from the overpower analysis. Any core geometry whose clad temperature exceeds temperature of the reference core cladding at any time will have its power reduced until it

no longer exceeds the reference clad temperature. This will determine the maximum power over the entire range of geometries for steady state, overpower, and LOCA conditions.

Lastly, the LOFA transient will be applied to the most desirable core geometries as determined by the previous analyses along with an economic analysis.

The power and flow history during the LOFA will be determined using RELAP and will be used as the input to VIPRE to determine the time step where the MDNBR is lowest.

Using the coast down values provided by RELAP the power and flow will be determined such that they meet they Safety Analysis Limit MDNBR of the reference core. This will then yield the Rated Power for this core geometry under LOFA conditions.

However, as the steady state power is decreased due to LOFA limitations, the mass flowrate will also be lowered, in order to maintain constant enthalpy rise across the core. The flow coastdown rate, however, is dependent up not only the core geometry but the initial mass flow rate as well. This is demonstrated in Appendix B. This makes it necessary to iterate between the flow coastdown value obtained from RELAP and the steady state power (and thus flow) obtained from VIPRE until the coastdown value and power yield the same flow that value within 1%.

This iteration provides a final maximum power and flow for each geometry such that they meet all the limits as previously proscribed in the steady state approach as well as the new $MDNBR_{S.A.L., REF}$ limit from the LOFA transient analysis.

This final Rated Power yields the maximum achievable power of the each core, considering both steady state, overpower, LOCA, and LOFA conditions.

BWR STEADY STATE LIMITS

3.1 – Common Assumptions

The modeling of all the core types examined throughout the analysis requires several VIPRE input files which contain all the necessary input data that describe the core geometry and the thermal-hydraulic conditions. Whenever one encounters:

- a parameter too complex to be exactly modeled and/or
- reduced interest in a particular nuclear aspect

the analysis can be simplified by means of assumptions. They can be conveniently grouped in seven categories:

- core structure assumptions
- bundle structure assumptions
- pressure drop assumptions
- coolant flow assumptions
- power distribution assumptions
- critical power determination assumptions
- other assumptions and considerations

Each category contains a number of different assumptions. Some of them are so general as to be common with all the cases examined, while others differ strongly from case to case. Those shared by all cases are listed and briefly described below. Whenever a more detailed description is required it will be presented in Appendix E, using the same categorization and numbering with letters. Conversely, the assumptions specifically referred to the single cases are presented in the relevant sections.

Core structure assumptions

a) The core peripheral region included between the outermost bundle ring and the core shroud (dashed in the sketch aside) is modeled as completely blocked, i.e. no coolant flows axially through it.

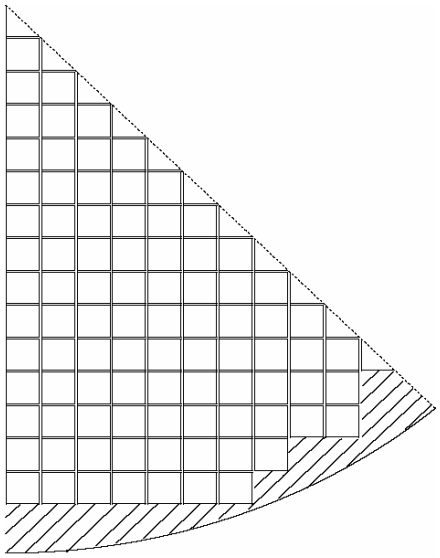

Figure 3.1: Peripheral Blocked Region

Bundle structure assumptions

a) The whole-core approach used to perform the analyses models 1/8th of the core, and each bundle as a single channel provided with a flow area, wetted and heated perimeter equal to the sum of the areas, wetted and heated perimeters of all the subchannels.

b) For the loss coefficient calculation, the grid spacers are assumed to have a thickness of 0.45 mm and height of 40 mm, which are typical values for these components.

c) The present analysis neglects the presence of Partial Length Fuel Rods (PLFRs), which are actually present both in the GE11 and in the GE14 fuel designs. All the rods contained in each assembly are assumed to be full length rods. Other than to simplify the analysis of the wide spectrum of bundle geometries assessed, this assumption is forced by the CPR correlation used, i.e. the Hench-Gillis correlation. It

is not suited to analyze bundles with PLFRs since it was developed using experimental data deriving from "old" bundle designs, which used only Full Length Fuel Rods. Moreover, if the whole core analysis accounted for the PLFRs, the J_1 factor entered in the whole core VIPRE input file would vary axially, but such an option is not permitted by the VIPRE code (see Section E1.1. in Appendix E for details).

Pressure drop assumptions

a) Although a real bundle has a total length larger than the heated length, this analysis was performed assuming they are equal. This is due to the VIPRE inability to predict correctly the power of each bundle. It has been verified that, both for whole core and subchannel analysis, when the two lengths are different VIPRE overestimates the thermal power of each bundle. Conversely, when the total length is set to be equal to the heated length the bundle power prediction is correct. However, because of the assumption made, the core pressure drop delivered by VIPRE is underestimated by a factor 1.046 for the BWR/5-type cores, and 1.131 for the ESBWR-type cores. Such multipliers are accounted for throughout the whole study, and all the core pressure drop values delivered by VIPRE are automatically multiplied by them. In such a way, the values calculated are representative of the real pressure drop characterizing the core types under examination.

b) The axial friction factor needed for the calculation of the pressure drop through the fuel bundles is determined from the Blasius relation:

$$f_F = a\,\mathrm{Re}^b \qquad \textbf{(3-1)}$$

where the coefficients a and b are computed by using the Cheng-Todreas friction factor correlations for square arrays having P/D $\geq$ 1.1 ([22]). See Table E.2 in Appendix E for the numerical values.

c) The form loss coefficient of the grid spacers is computed by a modified form of the In's correlation ([23]). See Appendix H for details.

Coolant flow assumptions

There are no assumptions common for all cases.

Power distribution assumptions

a) The axial power profile is assumed to be independent of the bundle radial position in the core. Thus, given a core type (BWR/5-type or ESBWR-type), all the bundles are assumed to have the same axial power profile. The power profiles used are described in the sections relative to each case.

b) Consistently with the lumping approach used for the subchannels forming each bundle, the radial power distribution inside them is not described in detail, i.e. the local peaking factors of each rod are not entered as input. However, the non-uniformity that characterizes the power distribution among the fuel rods is accounted for by entering, for each bundle[2], the maximum J_1 factor of the pin-by-pin power distribution under examination. A common pin-by-pin power distribution is considered for all the cases analyzed, regardless of the type of fuel and the bundle geometry. Such a power distribution is characterized by a maximum local peaking factor of 1.26 and a maximum J_1 factor of 1.198 located on a side rod (see Figure E.1). It is important to note that, because of the subchannel-lumping approach used, such an assumption does not mean that all the bundle designs examined throughout the analysis have the same fuel pin local peaking factors. Instead, it means that all the bundle designs are characterized by the same maximum localized non-uniformity in the pin-by-pin power distribution. Important comments about this assumption are presented in Section E1.1 of Appendix E.

Critical power determination assumptions

a) The calculation of the MCPR is performed by VIPRE using the Hench-Gillis correlation ([16], [4]). Important comments concerning the use of this relation are presented in Section E1.1. of Appendix E.

Other assumptions and considerations

[2] Since the pin-by-pin power distribution is assumed to be independent of the bundle position in the core, all the bundles have the same maximum J_1 factor.

a) The vibration ratio calculation was performed using the so-called *Païdoussis Corrected Correlation*. A detailed description of the approach used to analyze the vibration mechanisms in two-phase flow is presented in Appendix B. Except for those concerning the development of the vibration correlation itself, the main assumption made consists of analyzing the fuel rods as they were hollow tubes, i.e. neglecting the presence of the fuel and, for the hydride fueled rods, of the liquid metal (see next assumption). This is a conservative assumption since the absence of these heavy materials makes the rod weight smaller and therefore the vibrations amplitude larger. Moreover, the *Païdoussis Corrected Correlation* was not applied to the whole rod length, but only to the last section, that is the assembly portion included between the last grid spacer and the upper tie plate. In fact, because of the higher quality, this section is subjected to the most significant vibration motions. Given a core configuration, the calculation was performed for all the bundles, and the maximum vibration ratio calculated was compared with the limit value fixed in Table 2.3.

1.6 – Reference Parameters

The predicted core performance derived from the implementation of the new fuel type and/or from the modification of the lattice parameters *D* and *P*, will be often compared to those of two "reference cores". These "reference cores" do not exactly represent any existing core, although most of their features are in common with the General Electric BWR/5 of Nine Mile Point Unit 2 (NMP2), and with the recent GE ESBWR respectively[3]. This is basically due to the lack of some data which has been consequently replaced with values derived from different but consistent sources. For example, while parameters like the core power, coolant flow rate, number of bundles and system pressure for the two reference cores correspond exactly to those of NMP2 and of the ESBWR, the bundle geometries chosen are different. In fact, NMP2 is loaded with 8×8 assemblies ([7],

[3] The choice of the BWR/5 and the ESBWR as "reference reactors" was not made randomly. The former represents a model of an existing plant, for which the implementation of the hydride fuel, to be economically acceptable, should account for the presence of pre-existing structures and components, designed in view of an oxide-fueled core. Vice versa, the ESBWR represents a model of a future plant, for which the design of all the components is performed to accomodate hydride fuel. Since the ESBWR is not "pre-existing", its core can be designed with a greater freedom, such that all the potential advantages deriving from the use of the new fuel can be actually obtained.

Table 1.3-1) while the reference BWR/5 core contains 9×9 lattice assemblies (GE11 type), consistent with the current tendency to use bundles having a larger number of rods. It is important to stress that, in spite of the different number of rods, the fuel channel size is practically unchanged:

- NMP2 fuel channel size: 5.48×5.48 inches ([7], Table 1.3-1)
- GE11 fuel channel size: ~5.42×5.42 inches

Contrary to the choice made for the reference BWR/5 oxide core, the bundle design used for the reference ESBWR oxide core does not differ significantly from that actually designed for this reactor, i.e. the GE14 bundle design ([8]). Due to the incompleteness of the data sources, some of the bundle geometric characteristics refer to the GE14 design, while some others to the GE12 design. In spite of the different designations, the two designs are very similar.

Consistent with the nomenclature used for the two reference cores, the bundle designs modeled are called “reference bundle designs”, i.e. reference BWR/5 bundle and reference ESBWR bundle respectively.

The reference core key parameters are listed in Table 1.1.

Table 1.1: Reference Core Parameters				
Parameter	***Reference BWR/5***		***Reference ESBWR***	
	Value	***Source***	***Value***	***Source***
Core shroud radius, in (m)	102.56 (2.605)	[9]	120.36 (3.057)	Estimated from [10][4]
Number of fuel bundles	764	Table 1.3-1 in [7]	1132	Table 1.3-1 in [8]
Whole core flow rate, Mlbm/hr (kg/s)	108.5 (13671)	Table 4.4-1 in [11]	79.388 (10003)	Table 1.3-1 in [8]
System pressure, psia (MPa)	1035 (7.136)	Table 4.4-1 in [11]	1050 (7.240)	Table 4.4-1 in [8]
Core inlet temperature, F (ºC)	533 (278.3)	Table 4.4-1 in [11]	520 (271.1)	Table 4.4-1 in [8]
Thermal output power, MW	3323	Table 1.3-1 in [11]	4500	Table 1.3-1 in [8]

Figure 1.1 shows the GE11 fuel design, which was chosen as assembly design of the reference BWR/5 oxide core, and the GE14 bundle design, that the present analysis attempts to model approximately to use as the bundle design for the reference ESBWR core.

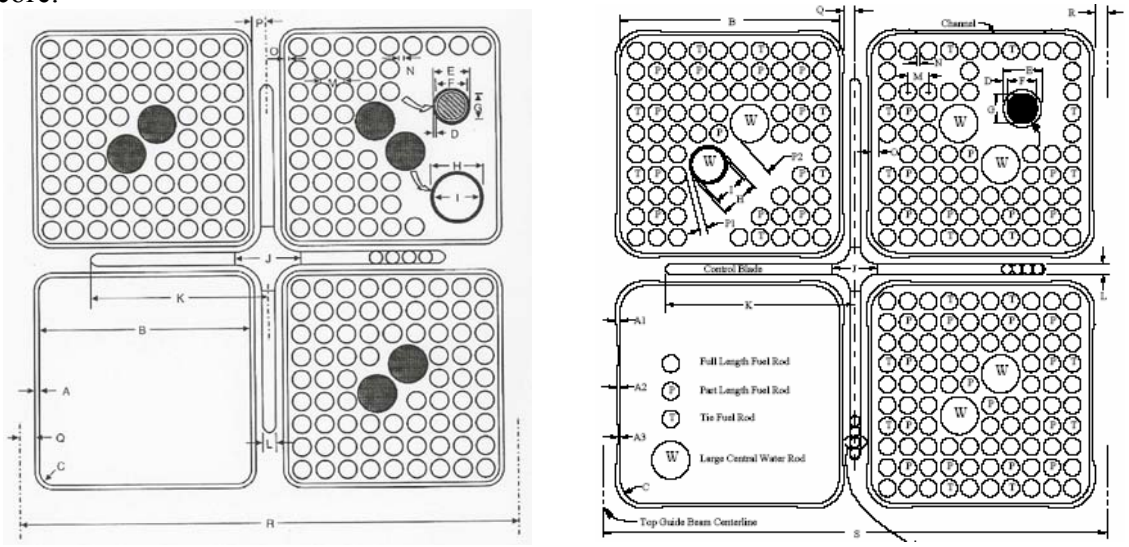

Figure 1.1: GE11 9×9 [12] and GE14 10×10 [13] Fuel Bundle Designs

[4] Figure 7 of [10] shows the overall ESBWR core layout. If a hypothetical infinite bundle array is assumed to occupy all the available space within the shroud, exactly 28 bundles would lie on the 45º symmetry line that diagonally cuts the core. Of these bundles, 26 are actually present, while the remaining two, i.e. the most peripheral ones, if present would touch the shroud inner surface with their upper left/bottom right corners respectively. Since the bundle pitch and the fuel channel outer width are known (P_b= 6.1" from [10], l_{bo} = 5.52" from Table 1.3-1 of [8]), the shroud radius can be calculated as: $R_{shroud}^{ESBWR} = 0.5 \cdot \left(27 \cdot \sqrt{2} \cdot P_b + \sqrt{2} \cdot l_{bo}\right) = 120.36"$.

Numerical values used for the two reference bundle designs are shown in Table 1.2. Most of the GE11 design values are not displayed since they are GE proprietary. Conversely, those used to represent the reference ESBWR fuel bundle derive from the coupling of GE12 and GE14 geometric data available in the open literature.

Table 1.2: Reference Assembly Key Parameters

	Reference BWR/5 bundle design (GE11-type)		***Reference ESBWR bundle design***	
	Value	***Source***	***Value***	***Source***
Number of fuel rods	74	[12]	92	[13]
Number of water rods	2		2	[13]
Fuel rod outer diameter, in (cm)	-		0.4039 (1.0260)	[14]
Fuel rod inner diameter, in (cm)	-		0.3441 (0.8740)	Calculated using clad thickness algorithms (see Section E1.3. of Appendix E)
Fuel pellet diameter, in (cm)	-		0.3386 (0.8600)	Calculated using gap thickness algorithms (see Section E1.3. of Appendix E)
Fuel rod pitch, in (cm)	-		0.5098 (1.2950)	[15]
Water rod outer diameter, in (cm)	-		1.0322 (2.6218)	Calculated using data in this table
Water rod wall thickness, in (cm)	-		-	Assumed to be the same as in GE11
Bundle outer width, in (cm)	-		5.52 (14.0208)	Table 1.3-1 of [8]
Bundle wall thickness, in (cm)	-		0.120 (0.3048)	Table 1.3-1 of [8]
Bundle active flow area, in^2 (cm^2)	-		14.4150 (93.0)	Table 4.4-1a of [8]
Bundle pitch, in (cm)	-		6.1 (15.4940)	[10]
Gap width between bundles, in (cm)	-		0.58 (1.4732)	Calculated using bundle pitch and bundle outer width

Geometric data used for all the core configurations analyzed, regardless of the values of the lattice parameters *D* and *P* and the type of fuel, are listed in Table 1.3.

Table 1.3: Key Bundle Geometric Data Used for All the Core Configurations				
	Cases adopting BWR/5-size vessel		***Cases adopting ESBWR-size vessel***	
Parameter	***Value***	***Source***	***Value***	***Source***
Fuel bundle total length, in (cm)	164.567 (418.0)	[3]	149.1 (378.7)	Table 1.3-1 in [8]
Fuel bundle heated length, in (cm)	145.98 (370.8)	[3]	120 (304.8)	Table 1.3-1 in [8]
Number of grid spacers	7	[15]	8	[15]

References

1. Ferroni, P. and N.E. Todreas, "Steady State Thermal Hydraulic Analysis of Hydride Fueled BWRs," MIT Dept. of Nuclear Science and Engineering, CANES Report MIT-NFC-PR-079, May 2006 (This report is identical to the M.S. thesis of P. Ferroni)
2. Shuffler, C., J. Trans, N. Todreas and A. Romano, "Application of Hydride Fuels to Enhance Pressurized Water Reactor Performance," MIT Dept. of Nuclear Science and Engineering, CANES Report MIT-NFC-TR-077, Jan. 2006 (This report combines the technical materials of the M.S. theses of C. Shuffler and J. Trant.)